Association of genetic variants in the *TMCO1* gene with clinical parameters related to glaucoma and characterisation of the protein in the eye

Running title: The TMCO1 gene and glaucoma

Shiwani Sharma[1]*, Kathryn P Burdon[1]*, Glyn Chidlow[2], Sonja Klebe[1,3], April Crawford[1], David P Dimasi[1] , Alpana Dave[1], Sarah Martin[1], Shahrbanou Javadiyan[1], John PM Wood[2], Robert Casson[2], Patrick Danoy[4], Kim Griggs[3], Alex W Hewitt[5], John Landers[1], Paul Mitchell[6], David A Mackey[5,7,8], Jamie E Craig[1]

1. Department of Ophthalmology, Flinders University, Flinders Medical Centre, Adelaide, Australia
2. South Australian Institute of Ophthalmology, Hanson Institute & Adelaide University
3. Department of Anatomical Pathology, Flinders University, Flinders Medical Centre, Adelaide, Australia
4. The University of Queensland Diamantina Institute, Princess Alexandra Hospital, Brisbane, Australia
5. Centre for Eye Research Australia, University of Melbourne, Royal Victorian Eye and Ear Hospital, Melbourne, Australia.
6.Centre for Vision Research, Department of Ophthalmology and Westmead Millennium Institute, University of Sydney, Westmead, Australia
7. Lions Eye Institute, University of Western Australia, Centre for Ophthalmology and Visual Science, Perth, Australia.
8. Discipline of Medicine, University of Tasmania, Hobart, Australia

* These authors contributed equally to this work

Word count: 4535

Funding sources: National Health and Medical Research Council of Australia, Glaucoma Australia and Ophthalmic Research Institute of Australia.

Abstract

Purpose: Glaucoma is the leading cause of irreversible blindness worldwide. Primary open angle glaucoma (POAG) is the most common sub-type. We recently reported association of genetic variants at chromosomal loci, 1q24 and 9p21, with POAG. In this study we determined association of the most significantly associated single nucleotide polymorphism (SNP) rs4656461, at 1q24 near the *TMCO1* gene, with the clinical parameters related to glaucoma risk and diagnosis, and determined ocular expression and sub-cellular localisation of the human TMCO1 protein to understand the mechanism of its involvement in POAG.

Methods: Association of SNP rs4656461 with five clinical parameters was assessed in 1420 POAG cases using linear regression. The *TMCO1* gene was screened for mutations in 95 cases with a strong family history and advanced disease. Ocular expression and sub-cellular localisation of the TMCO1 protein were determined by immunolabelling and as GFP-fusion.

Results: The data suggest that individuals homozygous for the rs4656461 risk allele (GG) are 4-5 years younger at diagnosis than non-carriers of this allele. Our data demonstrate expression of the TMCO1 protein in most tissues in the human eye including the trabecular meshwork and retina. However, the sub-cellular localisation differs from that reported in other studies. We demonstrate that the endogenous protein localises to the cytoplasm and nucleus *in vivo* and *ex vivo*. In the nucleus, the protein localises to the nucleoli.

Conclusions: This study shows a relationship between genetic variation in and around *TMCO1* with age at diagnosis of POAG and provides clues to the potential cellular function/s of this gene.

Introduction

Glaucoma refers to a group of neurodegenerative ocular diseases united by a clinically characteristic optic neuropathy. Open-Angle Glaucoma (OAG) is common, with a prevalence of around 3% in people over 50 years of age[1]. The disease has long been known to have a genetic component. First-degree relatives of affected patients exhibit a 9-fold increased relative risk of developing primary OAG (POAG) compared with the general population[2]. The Glaucoma Inheritance Study in Tasmania (GIST) revealed that a positive family history is found in approximately 60% of cases of POAG when family members are examined[3], and the disease is more severe in people with a family history of glaucoma, compared to those with "sporadic" glaucoma[4]. Mutations in the *myocilin* gene (*MYOC*) are the most common reported genetic cause of POAG and account for around 3%-5% of cases[5]. Mutations in *optineurin* (*OPTN*) and *WDR36* genes have also been implicated[5]. Recent genome-wide association studies have identified common variants at several new genetic loci are associated with POAG including *CAV1* and *CAV2* on chromosome 7q31, *CDKN2B-AS1*, *CDKN2A* and *CDKN2B* on 9p21, and *TMCO1* on 1q24[6, 7]. The mechanism of disease association is not yet clear for any of these genetic associations and very little is known about the normal function of *TMCO1* and its role in the eye.

The *TMCO1* gene encodes the Transmembrane and coiled-coil domains-1 protein which belongs to the DUF841 superfamily of unknown function[8]. The gene is located ~6Mb upstream of the known POAG gene *MYOC* on chromosome 1. The protein sequence is highly conserved across mammalian species[9]. The gene is expressed in a variety of human adult and fetal tissues at varying levels[9], including ocular tissues[6]. Immunohistochemistry revealed cytoplasmic labelling in the rat retinal ganglion cell layer[6]. The GFP (green fluorescent protein)-fusion of TMCO1 has been reported to localise to endoplasmic reticulum and Golgi

apparatus in COS7 cells[10], and to the mitochondria in porcine PK-15 cells[8]. These reports suggest that the sub-cellular localisation of the protein may differ depending on cell type. A homozygous frame-shift mutation in the *TMCO1* gene has been shown to cause a rare recessive syndrome in the Amish consisting of craniofacial dysmorphism, skeletal anomalies and mental retardation, now known as 'TMCO1 defect syndrome' [9]. There are no reports of glaucoma in this family. Our recent study failed to find any coding mutations in POAG patients carrying two risk haplotypes at the *TMCO1* locus, indicating that coding mutations in *TMCO1* are unlikely to account for the association observed with POAG[6].

The most associated SNP at the 1q24 locus (rs4656461) is just 3' to *TMCO1* and the second ranked SNP rs7518099 is within intron 2 of this gene and is in almost complete linkage disequilibrium with rs4656461. In addition, the highest ranked imputed SNP, rs7524755 is within the 3' UTR of *TMCO1*[6]. All the associated SNPs are within the same linkage disequilibrium block as *TMCO1* with no other transcripts in the block. The common haplotype across the gene, which is efficiently tagged by the most associated SNP, increases the risk of POAG. This association was discovered in a cohort of POAG patients with severe blinding disease, replicated in a second similar cohort and another cohort with less-severe glaucoma[6]. From these data, however, it is as yet unclear whether *TMCO1* genetic variation can be used to pinpoint a distinct sub-type of POAG or if *TMCO1* mutations might contribute to some cases of familial OAG.

In the present study, we further investigated the *TMCO1* gene for association with clinical traits relevant to glaucoma risk and diagnosis, and screened for mutations in patients with a strong family history of POAG. In addition, we investigated the detailed expression pattern of *TMCO1* in human eye and determined the sub-cellular localisation of the protein in relevant cell lines and *in vivo* in the eye.

Methods

Patient recruitment and data collection

Participants were drawn from the Australian & New Zealand Registry of Advanced Glaucoma (ANZRAG), the GIST, the Blue Mountains Eye Study (BMES) and patients attending the eye clinic at Flinders Medical Centre (Adelaide, Australia). All participants were included in the study reporting the association of *TMCO1* with POAG and the cohorts are described in more detail in that report[6]. This cohort was also examined for genotype-phenotype relationships at another POAG locus on chromosome 9p21 in an independent study[11]. POAG was defined by concordant findings of typical glaucomatous visual field defects on the Humphrey 24-2 test (Humphrey 30-2 test was used in BMES), with corresponding optic disc rim thinning, including an enlarged cup-disc ratio (≥ 0.7), or cup-disc ratio asymmetry (≥0.2) between the two eyes. Clinical exclusion criteria were: i) pseudoexfoliation or pigmentary glaucoma, ii) angle closure or mixed mechanism glaucoma, iii) secondary glaucoma due to aphakia, rubella, rubeosis or inflammation, iv) infantile glaucoma, and v) glaucoma in the presence of a known associated syndrome. Available clinical data were extracted from each study, and included sex, age at diagnosis, highest recorded intraocular pressure (IOP), visual field mean deviation, vertical cup:disc ratio, central corneal thickness and genotype at SNP rs4656461. Where full clinical records were available, age at diagnosis was defined as the first occasion on which the patient demonstrated definitive glaucomatous visual field loss, as defined in the inclusion criteria. When this information was not available, the chronological age of the patient at the initiation of treatment for glaucoma (eye drops, laser or surgery) was taken. All participants provided written informed consent. Approval was obtained from the Human Research Ethics Committees (HRECs) of Southern Adelaide Health Service/Flinders

University, University of Tasmania and The Royal Victorian Eye and Ear Hospital. All participants were screened for mutations in the *MYOC* gene by direct sequencing of exon 3 on an ABI PRISM 3100 Genetic Analyzer (Applied Biosystems, Foster City, CA, USA) with BigDye Terminators (Applied Biosystems, Foster City, CA, USA) according to standard protocols. Primer sequences are available on request.

Genotyping and association analysis

Genotyping of the rs4656461 SNP was conducted as previously reported[6]. Briefly, samples originally included in the discovery phase of the genome-wide association scan were genotyped on Omni1 SNP arrays (Illumina Inc, San Diego, CA, USA) while those included in the replication phase were typed with iPlex Gold chemistry on an Autoflex Mass Spectrometer (Sequenom Inc. San Diego, CA, USA). Each clinical trait was assessed for association with SNP rs4656461 (the glaucoma-associated SNP tagging the at-risk haplotype as reported previously[6]) using linear regression under a dominant genetic model. This model was chosen to maintain statistical power because this SNP is relatively rare (minor allele frequency ~12%) and only 24 homozygous patients were observed in our cohort. SNP genotypes were coded as carriers of the POAG risk allele (GA or GG genotype) and non-carriers (AA genotype), and analysed in the model as a categorical variable. The assumptions of linear regression were met. A p-value of 0.01 was required to account for the multiple testing of 5 traits (highest recorded IOP, age at diagnosis, mean deviation, cup:disc ratio and central corneal thickness). Significantly associated traits were then assessed under multivariate analysis including each of the other traits as well as sex in the model. Analyses were conducted including and excluding patients with known *MYOC* mutations. All analyses were conducted using IBM-SPSS Statistics V19 (IBM Corp, Armonk, NY, USA).

Sequencing of the TMCO1 gene

Ninety-five participants from the ANZRAG and GIST with advanced POAG (defined as best-corrected visual acuity worse than 6/60 due to POAG, or a reliable 24-2 Visual Field with a mean deviation of worse than -22db or at least 2 out of 4 central fixation squares affected with a Pattern Standard Deviation of < 0.5%) and a strong family history of POAG were selected for re-sequencing of the protein coding regions of the *TMCO1* gene. Family history was defined as three or more relatives diagnosed with glaucoma. This was self-reported in ANZRAG but determined by ophthalmic examination of extended families in GIST. Each exon and flanking intron of the *TMCO1* gene was sequenced as previously described[6]. Sequences were compared to the *TMCO1* reference sequence (GenBank Accession NM_019026) using Sequencher V4.10.1 (GeneCodes Corporation, Ann Arbor, MI, USA).

Subcellular localisation

A GFP-TMCO1 fusion construct was generated by cloning the open-reading frame of the protein in pEGFP-C1 (Clontech Laboratories, Inc, Mountain View, CA, USA). For this, *TMCO1* cDNA was amplified from the human retina as previously described[6] and cloned in-frame with GFP at *Eco*RI and *Xba*I sites in the vector. In-frame cloning was confirmed by sequencing. Expression of the fusion protein was demonstrated in transiently transfected HEK293A cells by Western blotting as previously described[12] except that protein extraction was performed in RIPA buffer [10 mM HEPES pH7.5, 150 mM NaCl, 1% Triton X-100, 0.5% sodium deoxycholate, 0.1% SDS, 2 mM EDTA, Protease Inhibitor Cocktail (Roche Diagnostics), 57 μM PMSF, 2 mM sodium orthovanadate, 10 mM sodium pyrophosphate and 20 mM sodium fluoride]. For subcellular localisation, 3×10^5 SH-SY5Y human neuroblastoma cells were seeded onto glass coverslips in 6-well tissue culture plates. The cells were cultured in a 1:1 mixture of Dulbecco's modified Eagle's medium and Ham's F12 medium (GIBCO,

Invitrogen Australia Pty Ltd, Mulgrave, Vic) supplemented with 10% fetal bovine serum and 1% penicillin/streptomycin, in a humidified atmosphere at 37°C and 5% CO2. On the following day, the cells were transfected with either GFP-TMCO1 fusion construct or empty vector using Lipofectamine 2000 (Invitrogen Australia Pty Ltd) as per the manufacturer's protocol. Approximately 48h post-transfection, the cells were incubated with 1μM BODIPY-TR-Ceramide (Molecular Probes, Invitrogen Australia Pty Ltd) for 2h to label the golgi apparatus or with 0.25μM MitoTracker® Red CM-H_2XRos (Molecular Probes) for 30 min to label mitochondria. After incubation, the cells were washed several times with phosphate buffered saline (PBS), fixed in 4% paraformaldehyde/PBS, and mounted on microscope slides in ProLong® Gold antifade reagent with DAPI (Molecular Probes). Confocal microscopy was performed on a Leica TCS SP5 inverted Spectral confocal microscope equipped with LAS AF software.

Immunolabelling

For immunohistochemical labelling of the TMCO1 protein in human eye, the eye tissue was obtained from deceased donors through the Eye Bank of South Australia, following the guidelines of the Southern Adelaide Health Service/Flinders University HREC. The tissue was obtained within 12 hours of donor death and average donor age was 70 years. The tissue from donors without a history of ocular disease such as keratoconus, pterygium, refractive surgery, inflammation, tumor and glaucoma, was obtained. Specificity of the rabbit anti-human TMCO1 antibody (Sigma-Aldrich, Pty Ltd, Castle Hill, NSW, Australia) used for immunolabelling was demonstrated in human optic nerve by Western blotting as previously described[13]. For immunolabelling, the eye tissue was fixed in buffered-formalin and embedded in paraffin. 4 μm thick paraffin embedded sections of the human eye were immunolabelled for the TMCO1 protein as previously described[14] except for the following

variations. After hybridisation with the rabbit anti-human TMCO1 primary antibody (1:1000), the sections were hybridised with the NovoLink® Polymer complex reagent (Leica Microsystems, Bannockburn, IL, USA) and visualised by Chromogen substrate coloration (Dako, Glostrup, Denmark). Sections were counterstained with haematoxylin and mounted in DePeX (Merck KGaA, Darmstadt, Germany). Light microscopy was performed on an Olympus BX41 microscope attached with a digital DP20/DP70 camera using CellSens Standard Photography software (Olympus Corporation, Tokyo, Japan).

Double immunofluorescent labelling in human eye sections was performed as previously described[15]. Visualisation of nucleolin, coilin and SC35 was achieved using a 3-step procedure (primary antibody, biotinylated secondary antibody, streptavidin-conjugated AlexaFluor 594), while TMCO1 was labelled by a 2-step procedure (primary antibody, secondary antibody conjugated to AlexaFluor 488). In brief, tissue sections were deparaffinized. Next, antigen retrieval was achieved by microwaving the sections in 10 mM citrate buffer (pH 6.0). Tissue sections were then blocked in PBS containing 3% normal horse serum and subsequently incubated overnight at room temperature in the appropriate combination of primary antibodies. On the following day, sections were incubated with biotinylated anti-mouse secondary antibody (1:250) for the 3-step procedure plus the anti-rabbit secondary antibody conjugated to AlexaFluor 488 (1:250, Molecular Probes) for the 2-step procedure for 30 min, followed by streptavidin-conjugated AlexaFluor 594 (1:500, Molecular Probes) for 1h. Sections were then mounted using anti-fade mounting medium and examined under a confocal fluorescence microscope. The following antibodies were used: rabbit anti-human TMCO1 (ARP49429, Aviva Systems Biology, San Diego, CA. USA), mouse anti-human nucleolin (ab13541, Abcam, Cambridge, MA, USA), mouse anti-human coilin (ab11822, Abcam), mouse anti-SC35 (ab11826 Abcam).

For immunolabelling of endogenous TMCO1 in SH-SY5Y cells, 3×10^5 cells were seeded onto glass coverslips in 6-well plates. Three days later, labelling was performed as previously described[12]. The cells were hybridised with the rabbit anti-TMCO1 primary antibody (1:1000; Sigma) followed by hybridisation with the Alexa Flour 488 conjugated anti-rabbit IgG secondary antibody (1:1000; Molecular Probes). For double labelling, the cells were hybridised with the anti-TMCO1 antibody and mouse anti-nucleolin monoclonal antibody (1:500; Abcam). The anti-TMCO1 antibody was detected with Alexa Flour 488 conjugated anti-rabbit IgG secondary antibody and anti-nucleolin with Alexa Fluor 594 conjugated anti-mouse IgG secondary antibody (1:500; Molecular Probes). The single and double labelled cells were mounted, and confocal microscopy performed as described above.

Results

Characterisation of the glaucoma phenotype associated with TMCO1 genetic variants

Genotype information for SNP rs4656461 and clinical characterisation of the disease were available for 1420 individuals. Descriptive statistics of each measured clinical trait are given in Table 1. For some individuals, the data for some of the clinical traits was not available. Each clinical trait was assessed for association with SNP rs4656461 (Table 2). Age at diagnosis was significantly decreased in carriers of the POAG risk allele (G) at this SNP (p=0.004). Vertical cup:disc ratio was increased (p=0.017); however, this result did not survive Bonferroni correction for the five traits assessed and the effect size estimate was small. Exclusion of 20 patients carrying pathogenic mutations in the *MYOC* gene did not significantly alter the results.

To explore the relationship between SNP rs4656461 and age at diagnosis further, multiple linear regression was conducted, including additional clinical covariates in the model. Carriers of POAG risk alleles were diagnosed over 3 years earlier than patients with no risk alleles at this locus (p=0.024, Table 3). Highest recorded IOP also contributed significantly to the model with a higher IOP also leading to a slightly younger age at diagnosis (0.26 years, p=0.0002). Exclusion of patients with *MYOC* mutations improved the significance of the observed association with age at diagnosis. The B coefficient increased to -3.54 (p=0.011), indicating a slightly stronger relationship when these generally young age at diagnosis patients were removed. In the multivariate analysis, the association with IOP was still significant but slightly attenuated with the exclusion of *MYOC* carriers (B=-0.243, p=0.001). The mean age at diagnosis by genotype of rs4656461 is shown in Table 4. Consistent with the multivariate model, the mean age at diagnosis was decreased 2-3 years for each POAG risk allele in the total cohort. This is also evident when *MYOC* carriers are excluded. No significant association of rs4656461 with age at diagnosis was observed in the *MYOC* mutation carriers (ANOVA p=0.971). The borderline association with cup:disc ratio was not significant after inclusion of IOP, age at diagnosis, CCT and sex in the model (p=0.066, data not shown).

Of 320 carriers of the rs4546461 risk allele (G), 60% (n=195) reported a family history of glaucoma. By comparison only 51% of non-carriers (331 of 643) reported a family history. This demonstrates an enrichment for family history of glaucoma amongst *TMCO1* risk allele carriers (OR=1.47, 95%CI [1.12-1.93], p=0.007). In order to identify heritable rare variants that may contribute to the POAG phenotype, 95 patients with a strong family history of the disease were selected for re-sequencing of the gene. Although several previously reported

SNPs, present in the general population, were observed, no novel pathogenic mutations were detected in the protein coding regions of the gene in this subset of individuals.

Sub-cellular localisation of TMCO1 and expression in mammalian eye

To explore the subcellular localisation of the TMCO1 protein in cell lines relevant to the retina, GFP-TMCO1 fusion was transiently expressed in SH-SY5Y human neuroblastoma cells. Prior to that, expression of the fusion protein by the fusion construct in HEK293A cells was demonstrated by Western blotting (Figure 1A). In SH-SY5Y cells the fusion protein was found either uniformly distributed in the cytoplasm or concentrated around the nucleus or aggregated on one side of the nucleus (Figure 1B and data not shown). However, labelling of these cells with the golgi apparatus or mitochondrial marker did not show any co-localisation of the protein with either organelle (Figure 1B, top and middle panels). In GFP expressing control cells, the protein distributed throughout the cell and, as expected, did not co-localise with the golgi apparatus or mitochondria (Figure 1B, bottom panels). A similar localisation pattern of the GFP-TMCO1 fusion was seen in SRA 01/04 lens epithelial cells (data not shown).

For determining expression and *in vivo* localisation of TMCO1 in the human eye, immunolabelling was performed in human ocular sections with the anti-TMCO1 antibody. Specificity of the antibody was demonstrated by detection of the expected ~21 kDa protein band in human optic nerve by Western blotting (Figure 2A). In human ocular sections, positive immunolabelling was observed in the iridocorneal angle, trabecular meshwork, ciliary body and retina (Figure 2B). In the trabecular meshwork, positive immunolabelling was primarily seen as 1-2 dots in the nucleus along with cytoplasmic labelling (Figure 2B-B and C). A similar pattern of nuclear labelling and cytoplasmic labelling was observed in cells in the ciliary body (Figure 2B-D and E). In the retina, dot-like nuclear and positive

cytoplasmic labelling was observed in the photoreceptor, bipolar and ganglion cell layers (Figure 2B-F and G). Cytoplasmic labelling was more prominent in the photoreceptor outer segments and ganglion cells than in bipolar cells. These data suggest that the TMCO1 protein is expressed in most ocular tissues and corroborate the previous finding of *TMCO1* transcript in these tissues[6]. Cytoplasmic labelling correlates with that previously reported by us in rat retinal ganglion cells[6]. Nuclear and cytoplasmic labelling of the protein in the eye indicates that TMCO1 is likely a multifunctional protein with functions both in the cytoplasm and nucleus. However, as all nuclear proteins are produced in the cytoplasm and then translocated to the nucleus, it is possible that the cytoplasmic labelling of TMCO1 represents its production rather than function in this compartment.

Next, we investigated the identity of the discrete sub-nuclear regions immunopositive for TMCO1 in the cells in ocular tissues. We hypothesised that these sub-nuclear regions either represent nucleoli, Cajal body or nuclear speckles. Nucleolin is a protein that frequently localises to the nucleoli and is therefore used as a nucleolar marker[16]. However it is also known to localise to the perinucleolar compartment[17]. The coilin protein markers the Cajal body and SC35 the speckles in the nucleus[18]. To determine whether TMCO1 localises to the nucleolus, Cajal body or speckles in the cells in ocular tissues, we individually assessed its co-localisation with nucleolin, coilin and SC35 proteins. Double labelling with the anti-TMCO1 and anti-nucleolin antibodies revealed co-localisation of TMCO1 and nucleolin in the nucleus to discrete sub-cellular regions in the cells in human ocular sections. Representative co-localisation in the retinal ganglion cells can be seen in Figure 3. The two proteins were also observed in the cytoplasm in ocular cells where they co-localised with each other. However, double labelling with anti-TMCO1 and anti-coilin antibodies and with anti-TMCO1 and anti-SC35 antibodies revealed that TMCO1 did not co-localise with coilin or

SC35 in the nucleus or cytoplasm (Figure 3). These data indicate that sub-nuclear TMCO1 in the cells in ocular tissues localises to nucleoli.

Finally, we investigated whether endogenous TMCO1 in SH-SY5Y cells mimics *in vivo* localisation in the human eye. Immunolabelling with the anti-TMCO1 antibody revealed distribution of the protein in the cytoplasm and nucleus in a punctate fashion in these cells (Figure 4, bottom left panel). The signal was stronger in the nucleus compared to the cytoplasm. In addition, in a small proportion of cells, instead of being evenly distributed in the nucleus the protein was concentrated to discrete sub-nuclear regions as seen *in vivo* in the eye (Figure 4, top left panel). To determine if these TMCO1 positive sub-nuclear regions represent nucleoli, we assessed co-localisation of TMCO1 with nucleolin in SH-SY5Y cells. Double labelling with the anti-TMCO1 and anti-nucleolin antibodies revealed TMCO1 localisation as described above, and localisation of nucleolin to discrete sub-nuclear regions (Figure 4, second column). In cells with sub-nuclear localisation of TMCO1, the protein showed complete co-localisation with nucleolin in some cells (Figure 4, top row), as observed *in vivo*, and exhibited incomplete co-localisation in other cells (Figure 4, middle row). In cells where TMCO1 was evenly distributed in the nucleus, the protein did not co-localise with nucleolin (Figure 4, bottom row). Double labelling with anti-TMCO1 and anti-coilin and with anti-TMCO1 and anti-SC35 antibodies showed that TMCO1 does not co-localise with coilin or SC35 in SH-SY5Y cells (data not shown). From these data TMCO1 appears to shuttle between the cytoplasm and nucleus and transiently localise to the nucleolus or the perinucleolar compartment.

Discussion

Genetic variation in and around the *TMCO1* gene at 1q24 has been shown to be associated with POAG[6]. The function of this gene is not well elucidated and it is not yet known how this

gene contributes to glaucoma. This study has shown that POAG patients carrying the glaucoma risk alleles at SNP rs4656461 tend to be diagnosed with the disease several years earlier than patients without these alleles. However, this study was not able to show association of rs4656461 with IOP, cup:disc ratio, mean deviation or central corneal thickness. Thus, apart from a slightly earlier onset, *TMCO1*-related glaucoma does not appear to be a clinically distinct sub-type of POAG. These SNPs may be severity factors for POAG, which could influence the age at onset of disease. This idea is consistent with our previous work showing an increased odds ratio for association in patients with blinding POAG compared to patients with less severe POAG[6]. In patients with a family history of advanced glaucoma, there may be a tendency for increased monitoring and thus earlier diagnosis (pseudo-anticipation). This phenomenon may contribute to the current findings given the observation of an increased family history in risk allele carriers. This is a limitation of our approach, however, the same association with age of diagnosis was not observed at the *CDKN2B-AS1* gene in this same cohort [11]. Thus, we believe pseudo-anticipation is not having a major effect on the current findings.

MYOC glaucoma is also well known to have a younger age of onset, but within this small group of patients the *TMCO1* gene does not appear to be modifying this risk although the power of this analysis is minimal in this cohort with a limited number of participants carrying both *MYOC* mutations and *TMCO1* risk alleles. The inclusion of patients with *MYOC* mutations in the current analysis also does not account for the younger age of diagnosis observed in *TMCO1* risk allele carriers. The methods used for the collection of age at diagnosis data do have some limitations. Where complete clinical records were not available to confirm the age of definitive glaucomatous visual loss, self reported age at treatment initiation was used as a surrogate. However, it is unlikely that any bias introduced by this

limitation would be distributed differently across genotypes. Nevertheless, replication of the observed association in independent POAG cohorts is required to confirm the current findings.

By re-sequencing of 95 patients with a strong family history of POAG, coding variants do not appear responsible for the disease phenotype in these families deemed likely to have highly penetrant dominant mutations. This is not surprising given that the amino acid sequence of this protein is completely conserved between all mammals investigated to date[9]. This implies a crucial role for this ubiquitously expressed protein. The absence of coding variants in POAG patients in this study suggests genetic variation in regulatory elements may be responsible for the observed association signal. Further in-depth and functional analysis of the locus is required to determine this.

As an initial step towards functional analysis of the *TMCO1* gene, we determined sub-cellular localisation of the encoded protein and protein expression in the human eye. Expression of the protein in all the ocular tissues is consistent with its reported ubiquitous expression[9]. Localisation of the GFP-TMCO1 fusion in cultured mammalian cells in this study contradicted the previous reports. Iwamuro *et al.* reported localisation of the human TMCO1-GFP fusion to the endoplasmic reticulum and golgi apparatus in COS-7 cells but did not determine co-localisation with the organelle specific markers[10]. Zhang *et al.*, however, reported localisation of the GFP fusion of porcine TMCO1 to mitochondria in PK-15 porcine kidney cells and co-localisation with the mitochondrial marker[8]. In this study, we observed neither co-localisation of human GFP-TMCO1 with the endoplasmic reticulum and golgi apparatus, nor mitochondria in cultured human neuroblastoma and lens epithelial cells. In addition, the fusion protein did not co-localise with the golgi apparatus or distribute to the endoplasmic reticulum in COS-7 cells under our experimental conditions (data not shown),

which further contradicts findings in these cells by Iwamuro *et al*[10]. Furthermore, we observed cytoplasmic and nuclear localisation as inclusions of endogenous TMCO1 in the human ocular tissues. In SH-SY5Y neuroblastoma cells also, endogenous TMCO1 was found in the cytoplasm and nucleus and in some cells as nuclear inclusions. Together, our data suggest that GFP-TMCO1 fusion localises differently than endogenous TMCO1. This may be because TMCO1 protein is smaller than GFP (~21 versus 28 kDa) thus the latter leads to aberrant localisation of the former or due to overexpression of the fusion protein. Grossly different localisation patterns of the GFP fusion and endogenous protein seen in this study highlight that ectopically expressed GFP fusions may not always reflect biological localisation of the protein of interest.

The functional significance of the cytoplasmic localisation of endogenous TMCO1 is as yet unclear. However, the conspicuous sub-nuclear localisation *in vivo* in the human eye and *ex vivo* in some SH-SY5Y cells, and co-localisation with nucleolin is very interesting. Nucleolin, the major component of the nucleolus, also localises to the perinucleolar compartment, nucleoplasm, and the cell surface[17, 19]. The nucleolus is conventionally involved in ribosome biogenesis but also has non-conventional roles including regulation of tumor suppressor and oncogene activities, nuclear export and control of aging[20]. The perinucleolar compartment is associated with malignancy[17]. Interestingly, the *CDKN2B* gene and the antisense RNA gene *CDKN2B-AS1* recently associated with POAG by us and others are involved in tumor suppression and cell-cycle regulation[6, 21]. From the present data it is not unreasonable to speculate that *TMCO1* may also play a role in tumor suppression and/or cell-cycle regulation. Furthermore, involvement of the nucleolus in controlling aging and association of the risk allele of SNP rs4656461 near the *TMCO1* gene with earlier age at diagnosis of glaucoma raise the possibility of a role of this gene in aging. In our view, this gene is likely involved in cell

cycle regulation in glaucoma. In conclusion, the present study provides clues to the potential cellular function/s of *TMCO1* and shows a relationship between genetic variation in and around this gene with age at diagnosis of POAG. It also suggests that SH-SY5Y cells are a useful model for investigating *TMCO1* function. Further longitudinal studies will investigate whether *TMCO1* genotyping can predict severity or progression of glaucoma.

Acknowledgements

This work was funded by the National Health and Medical Research Council (NHMRC) of Australia, Glaucoma Australia and Ophthalmic Research Institute of Australia. K.P.B is supported by the NHMRC Career development Award and J.E.C. by the Practitioner Fellowship.

References

1. Mitchell P, Smith W, Attebo K, Healey PR. Prevalence of open-angle glaucoma in Australia. The Blue Mountains Eye Study. Ophthalmology. 1996; 103:1661-9.
2. Wolfs RC, Klaver CC, Ramrattan RS, van Duijn CM, Hofman A, de Jong PT. Genetic risk of primary open-angle glaucoma. Population-based familial aggregation study. Archives of ophthalmology. 1998; 116:1640-5.
3. Green CM, Kearns LS, Wu J, Barbour JM, Wilkinson RM, Ring MA, Craig JE, Wong TL, Hewitt AW, Mackey DA. How significant is a family history of glaucoma? Experience from the Glaucoma Inheritance Study in Tasmania. Clin Experiment Ophthalmol. 2007; 35:793-9.
4. Wu J, Hewitt AW, Green CM, Ring MA, McCartney PJ, Craig JE, Mackey DA. Disease severity of familial glaucoma compared with sporadic glaucoma. Archives of ophthalmology. 2006; 124:950-4.
5. Allingham RR, Liu Y, Rhee DJ. The genetics of primary open angle glaucoma: A review. Exp Eye Res. 2009; 88:837-44.
6. Burdon KP, Macgregor S, Hewitt AW, Sharma S, Chidlow G, Mills RA, Danoy P, Casson R, Viswanathan AC, Liu JZ, Landers J, Henders AK, Wood J, Souzeau E, Crawford A, Leo P, Wang JJ, Rochtchina E, Nyholt DR, Martin NG, Montgomery GW, Mitchell P, Brown MA, Mackey DA, Craig JE. Genome-wide association study identifies susceptibility loci for open angle glaucoma at TMCO1 and CDKN2B-AS1. Nat Genet. 2011; 43:574-8.
7. Thorleifsson G, Walters GB, Hewitt AW, Masson G, Helgason A, Dewan A, Sigurdsson A, Jonasdottir A, Gudjonsson SA, Magnusson KP, Stefansson H, Lam DS, Tam PO, Gudmundsdottir GJ, Southgate L, Burdon KP, Gottfredsdottir MS, Aldred

MA, Mitchell P, St Clair D, Collier DA, Tang N, Sveinsson O, Macgregor S, Martin NG, Cree AJ, Gibson J, Macleod A, Jacob A, Ennis S, Young TL, Chan JC, Karwatowski WS, Hammond CJ, Thordarson K, Zhang M, Wadelius C, Lotery AJ, Trembath RC, Pang CP, Hoh J, Craig JE, Kong A, Mackey DA, Jonasson F, Thorsteinsdottir U, Stefansson K. Common variants near CAV1 and CAV2 are associated with primary open-angle glaucoma. Nat Genet. 2010;

8. Zhang Z, Mo D, Cong P, He Z, Ling F, Li A, Niu Y, Zhao X, Zhou C, Chen Y. Molecular cloning, expression patterns and subcellular localization of porcine TMCO1 gene. Mol Biol Rep. 2010; 37:1611-8.

9. Xin B, Puffenberger EG, Turben S, Tan H, Zhou A, Wang H. Homozygous frameshift mutation in TMCO1 causes a syndrome with craniofacial dysmorphism, skeletal anomalies, and mental retardation. Proc Natl Acad Sci U S A. 2010; 107:258-63.

10. Iwamuro S, Saeki M, Kato S. Multi-ubiquitination of a nascent membrane protein produced in a rabbit reticulocyte lysate. J Biochem. 1999; 126:48-53.

11. Burdon KP, Crawford A, Casson RJ, Hewitt AW, Landers J, Danoy P, Mackey DA, Mitchell P, Healey PR, Craig JE. Glaucoma Risk Alleles at CDKN2B-AS1 Are Associated with Lower Intraocular Pressure, Normal-Tension Glaucoma, and Advanced Glaucoma. Ophthalmology. 2012; In press.

12. Sharma S, Ang SL, Shaw M, Mackey DA, Gecz J, McAvoy JW, Craig JE. Nance-Horan syndrome protein, NHS, associates with epithelial cell junctions. Hum Mol Genet. 2006; 15:1972-83.

13. Burdon KP, Sharma S, Hewitt AW, McMellon AE, Wang JJ, Mackey DA, Mitchell P, Craig JE. Genetic analysis of the clusterin gene in pseudoexfoliation syndrome. Mol Vis. 2008; 14:1727-36.

14. Sharma S, Chataway T, Burdon KP, Jonavicius L, Klebe S, Hewitt AW, Mills RA, Craig JE. Identification of LOXL1 protein and Apolipoprotein E as components of surgically isolated pseudoexfoliation material by direct mass spectrometry. Exp Eye Res. 2009; 89:479-85.

15. Chidlow G, Ebneter A, Wood JP, Casson RJ. The optic nerve head is the site of axonal transport disruption, axonal cytoskeleton damage and putative axonal regeneration failure in a rat model of glaucoma. Acta Neuropathol. 2011; 121:737-51.

16. Ginisty H, Sicard H, Roger B, Bouvet P. Structure and functions of nucleolin. J Cell Sci. 1999; 112 (Pt 6):761-72.

17. Pollock C, Huang S. The perinucleolar compartment. Cold Spring Harb Perspect Biol. 2010; 2:a000679.

18. Sleeman JE. Dynamics of the mammalian nucleus: can microscopic movements help us to understand our genes? Philos Transact A Math Phys Eng Sci. 2004; 362:2775-93.

19. Mongelard F, Bouvet P. Nucleolin: a multiFACeTed protein. Trends Cell Biol. 2007; 17:80-6.

20. Olson MO, Hingorani K, Szebeni A. Conventional and nonconventional roles of the nucleolus. Int Rev Cytol. 2002; 219:199-266.

21. Ramdas WD, van Koolwijk LM, Lemij HG, Pasutto F, Cree AJ, Thorleifsson G, Janssen SF, Jacoline TB, Amin N, Rivadeneira F, Wolfs RC, Walters GB, Jonasson F, Weisschuh N, Mardin CY, Gibson J, Zegers RH, Hofman A, de Jong PT, Uitterlinden AG, Oostra BA, Thorsteinsdottir U, Gramer E, Welgen-Lussen UC, Kirwan JF, Bergen AA, Reis A, Stefansson K, Lotery AJ, Vingerling JR, Jansonius NM, Klaver CC, van Duijn CM. Common genetic variants associated with open-angle glaucoma. Hum Mol Genet. 2011; 20:2464-71.

Table 1: Clinical characteristics of the cohort.

Clinical trait	N	Mean±SD or %(n)
Highest recorded IOP (mmHg)	1275	26.5 ± 10.0
Age at diagnosis (years)	1141	62.4 ± 14.0
Mean deviation (dB)	658	-17.8 ± 9.4
Cup:disc ratio	1146	0.87 ± 0.13
Central corneal thickness (μm)	693	518 ± 41
Gender (% Male)	1389	46.6% (647)

Abbreviations: IOP= intraocular pressure; SD = standard deviation

Table 2: Association of SNP rs4656461 with each clinical trait under a dominant model.

Clinical trait	B	Standard Error	P-value
Highest recorded IOP	0.07	0.60	0.908
Age at diagnosis	-2.56	0.88	**0.004**
Mean deviation	-0.58	0.77	0.465
Cup:disc ratio	0.02	0.008	**0.017**
Central corneal thickness	-1.43	3.29	0.665

p-value < 0.01 is considered significant.

Table 3: Multiple regression for age at diagnosis. R^2=0.068.

Clinical trait	B	Standard Error	P-value
Highest recorded IOP	-0.26	0.07	0.0002
Mean Deviation	-0.02	0.09	0.841
Cup:disc ratio	8.55	7.16	0.233
Central corneal thickness	-0.03	0.02	0.078
Gender	1.78	1.36	0.193
rs4656461 G allele carriers	-3.13	1.39	0.024

p-value < 0.01 is considered significant.

Table 4: Mean age at diagnosis (years) by rs4656461 genotype. The G allele at this SNP is the risk allele for glaucoma. Analysis on *MYOC* mutation carriers and non-carriers is also shown. Stddev= Standard Deviation

	All patients			*MYOC* carriers			Non-*MYOC* carriers		
Genotype	N	Mean age	stddev	N	Mean age	stddev	N	Mean age	stddev
AA	769	63.3	14.1	11	46.3	19.4	758	63.5	13.9
AG	351	60.9	13.7	5	48.6	14.8	346	61.0	13.6
GG	21	58.7	14.4	2	47.0	8.5	19	59.9	14.5

Figure legends

Figure 1. **A)** Fusion protein encoded by the GFP-TMCO1 construct. Cell lysates from HEK 293A cells transiently transfected with the fusion construct (GFP-TMCO1) or pEGFP-C1 vector (GFP) were analysed by Western blotting with the anti-GFP antibody. The band of approximately 50 kDa seen in the TMCO1-GFP lane corresponds with the expected size of the fusion protein and that of approximately 28 kDa in the GFP lane corresponds with the size of GFP. The >28 kDa protein band seen in the TMCO1-GFP lane may represent fusion protein degradation. Molecular sizes of the protein standards are indicated in kilodaltons (kDa). **B)** GFP-TMCO1 fusion localisation in SH-SY5Y human retinoblastoma cells. Cells transiently transfected with the fusion construct (GFP-TMCO1) or pEGFP-C1 vector (GFP) (green channel) were either stained with BODIPY-TR-Ceramide for labelling the golgi apparatus (Golgi) or MitoTracker® Red CM-H_2XRos for labelling mitochondria (Mito) (red channel), nuclei counterstained with DAPI (blue channel), and visualised by confocal microscopy. GFP-TMCO1 can be seen in the cytoplasm (green). However, in overlayed images from the three channels (Merge) it neither co-localises with the golgi apparatus nor mitochondria. In cells expressing GFP as a control, the protein distributed in the nucleus and cytoplasm.

Figure 2. A) Endogenous TMCO1 protein in human optic nerve. Protein lysate from optic nerve tissue were analysed by Western blotting with the rabbit anti-TMCO1 antibody. The ~21 kDa band corresponds with the expected size of the TMCO1 protein. Molecular sizes of the protein standards are indicated in kilodaltons (kDa). B) Immunolabelling of TMCO1 in the human eye. Paraffin sections of human eye were immunolabelled with the anti-TMCO1 antibody and imaged by light microscopy. Positive immunolabelling can be seen as red signal in the A) iridocorneal angle, B, C) trabecular meshwork, D, E) ciliary body and F, G) retina.

Nuclei are stained blue. Pigment in panels A, C and E is marked by the letter 'p'. Immunolabelling of TMCO1 as an intense spot in the nucleus can be seen in cells in the trabecular meshwork (C), ciliary body (E) and retina (G). Cytoplasmic immunolabelling is also visible in these tissues. Images are, A at 10×, B, D, F at 40× and C, E, G at 600×, original magnification. The presented results are representative of experiments on eyes from four independent donors.

Figure 3. Immunolabelling of TMCO1 with nucleolin, coilin and SC35 in human retina. Confocal microscopy was performed on sections immunolabelled with anti-TMCO1 (green) antibody together with either anti-nucleolin, anti-coilin or anti-SC35 antibodies (red). Nuclei (blue) were stained with DAPI. Images from the three colour channels overlayed (merge) for determining co-localisation. Top row, TMCO1 localised to discrete regions in the nucleus co-localises with nucleolin (highlighted by arrows). Middle row, TMCO1 does not co-localise with coilin (green and red separated in merged image). Bottom row, TMCO1 does not co-localise with SC35 (green and red distinct in merged image). Scale bar: 5 μm.

Figure 4. Immunolabelling of TMCO1 and nucleolin in human SH-SY5Y neuroblastoma cells. Confocal microscopy was performed on cells immunolabelled with the anti-TMCO1 (green) and anti-nucleolin (red) antibodies. Nuclei (blue) were stained with DAPI. Images from the three colour channels overlayed (merge) for determining co-localisation. Top row, TMCO1 localised to discrete regions in the nucleus co-localises with nucleolin (yellow in merged image). Middle row, TMCO1 although localised to discrete regions in the nucleus does not completely co-localise with nucleolin (green and red somewhat separated in merged image). Bottom row, TMCO1 evenly distributed in the nucleus does not co-localise with nucleolin (green and red distinct in merged image). Images were taken with a 63× objective.

Brightness and contrast of images in the bottom row were enhanced for improving visibility of the cytoplasmic signal.

Table 1: Clinical characteristics of the cohort.

Clinical trait	N	Mean±SD or %(n)
Highest recorded IOP (mmHg)	1275	26.5 ± 10.0
Age at diagnosis (years)	1141	62.4 ± 14.0
Mean deviation (dB)	658	-17.8 ± 9.4
Cup:disc ratio	1146	0.87 ± 0.13
Central corneal thickness (μm)	693	518 ± 41
Gender (% Male)	1389	46.6% (647)

Abbreviations: IOP= intraocular pressure; SD = standard deviation

Table 2: Association of SNP rs4656461 with each clinical trait under a dominant model.

Clinical trait	B	Standard Error	P-value
Highest recorded IOP	0.07	0.60	0.908
Age at diagnosis	-2.56	0.88	**0.004**
Mean deviation	-0.58	0.77	0.465
Cup:disc ratio	0.02	0.008	**0.017**
Central corneal thickness	-1.43	3.29	0.665

p-value < 0.01 is considered significant.

Table 3: Multiple regression for age at diagnosis. R^2=0.068.

Clinical trait	B	Standard Error	P-value
Highest recorded IOP	-0.26	0.07	0.0002
Mean Deviation	-0.02	0.09	0.841
Cup:disc ratio	8.55	7.16	0.233
Central corneal thickness	-0.03	0.02	0.078
Gender	1.78	1.36	0.193
rs4656461 G allele carriers	-3.13	1.39	0.024

p-value < 0.01 is considered significant.

Table 4: Mean age at diagnosis (years) by rs4656461 genotype. The G allele at this SNP is the risk allele for glaucoma. Analysis on *MYOC* mutation carriers and non-carriers is also shown. Stddev= Standard Deviation

	All patients			*MYOC* carriers			Non-*MYOC* carriers		
Genotype	N	Mean age	stddev	N	Mean age	stddev	N	Mean age	stddev
AA	769	63.3	14.1	11	46.3	19.4	758	63.5	13.9
AG	351	60.9	13.7	5	48.6	14.8	346	61.0	13.6
GG	21	58.7	14.4	2	47.0	8.5	19	59.9	14.5

Figure legends

Figure 1. **A)** Fusion protein encoded by the GFP-TMCO1 construct. Cell lysates from HEK 293A cells transiently transfected with the fusion construct (GFP-TMCO1) or pEGFP-C1 vector (GFP) were analysed by Western blotting with the anti-GFP antibody. The band of approximately 50 kDa seen in the TMCO1-GFP lane corresponds with the expected size of the fusion protein and that of approximately 28 kDa in the GFP lane corresponds with the size of GFP. The >28 kDa protein band seen in the TMCO1-GFP lane may represent fusion protein degradation. Molecular sizes of the protein standards are indicated in kilodaltons (kDa). **B)** GFP-TMCO1 fusion localisation in SH-SY5Y human retinoblastoma cells. Cells transiently transfected with the fusion construct (GFP-TMCO1) or pEGFP-C1 vector (GFP) (green channel) were either stained with BODIPY-TR-Ceramide for labelling the golgi apparatus (Golgi) or MitoTracker® Red CM-H_2XRos for labelling mitochondria (Mito) (red channel), nuclei counterstained with DAPI (blue channel), and visualised by confocal microscopy. GFP-TMCO1 can be seen in the cytoplasm (green). However, in overlayed images from the three channels (Merge) it neither co-localises with the golgi apparatus nor mitochondria. In cells expressing GFP as a control, the protein distributed in the nucleus and cytoplasm.

Figure 2. A) Endogenous TMCO1 protein in human optic nerve. Protein lysate from optic nerve tissue were analysed by Western blotting with the rabbit anti-TMCO1 antibody. The ~21 kDa band corresponds with the expected size of the TMCO1 protein. Molecular sizes of the protein standards are indicated in kilodaltons (kDa). B) Immunolabelling of TMCO1 in the human eye. Paraffin sections of human eye were immunolabelled with the anti-TMCO1 antibody and imaged by light microscopy. Positive immunolabelling can be seen as red signal in the A) iridocorneal angle, B, C) trabecular meshwork, D, E) ciliary body and F, G) retina.

Nuclei are stained blue. Pigment in panels A, C and E is marked by the letter 'p'. Immunolabelling of TMCO1 as an intense spot in the nucleus can be seen in cells in the trabecular meshwork (C), ciliary body (E) and retina (G). Cytoplasmic immunolabelling is also visible in these tissues. Images are, A at 10×, B, D, F at 40× and C, E, G at 600×, original magnification. The presented results are representative of experiments on eyes from four independent donors.

Figure 3. Immunolabelling of TMCO1 with nucleolin, coilin and SC35 in human retina. Confocal microscopy was performed on sections immunolabelled with anti-TMCO1 (green) antibody together with either anti-nucleolin, anti-coilin or anti-SC35 antibodies (red). Nuclei (blue) were stained with DAPI. Images from the three colour channels overlayed (merge) for determining co-localisation. Top row, TMCO1 localised to discrete regions in the nucleus co-localises with nucleolin (highlighted by arrows). Middle row, TMCO1 does not co-localise with coilin (green and red separated in merged image). Bottom row, TMCO1 does not co-localise with SC35 (green and red distinct in merged image). Scale bar: 5 μm.

Figure 4. Immunolabelling of TMCO1 and nucleolin in human SH-SY5Y neuroblastoma cells. Confocal microscopy was performed on cells immunolabelled with the anti-TMCO1 (green) and anti-nucleolin (red) antibodies. Nuclei (blue) were stained with DAPI. Images from the three colour channels overlayed (merge) for determining co-localisation. Top row, TMCO1 localised to discrete regions in the nucleus co-localises with nucleolin (yellow in merged image). Middle row, TMCO1 although localised to discrete regions in the nucleus does not completely co-localise with nucleolin (green and red somewhat separated in merged image). Bottom row, TMCO1 evenly distributed in the nucleus does not co-localise with nucleolin (green and red distinct in merged image). Images were taken with a 63× objective.

Brightness and contrast of images in the bottom row were enhanced for improving visibility of the cytoplasmic signal.

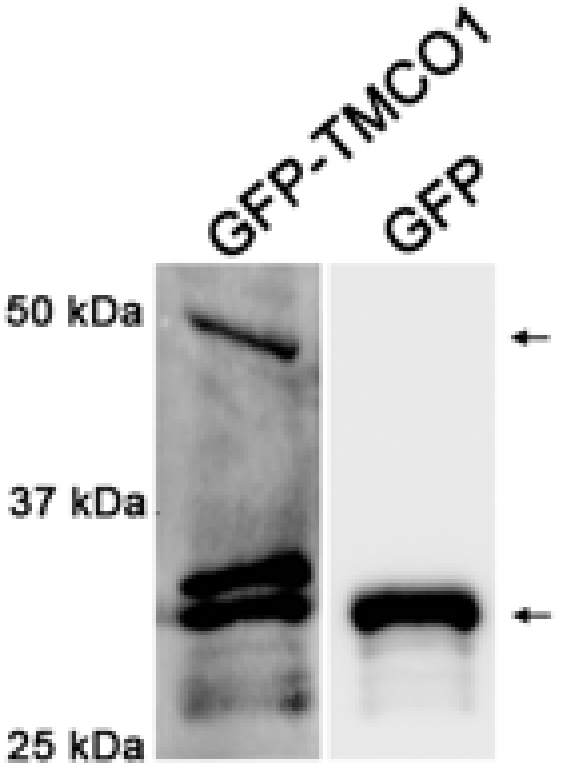
GFP-TMCO1
GFP
50 kDa
37 kDa
25 kDa

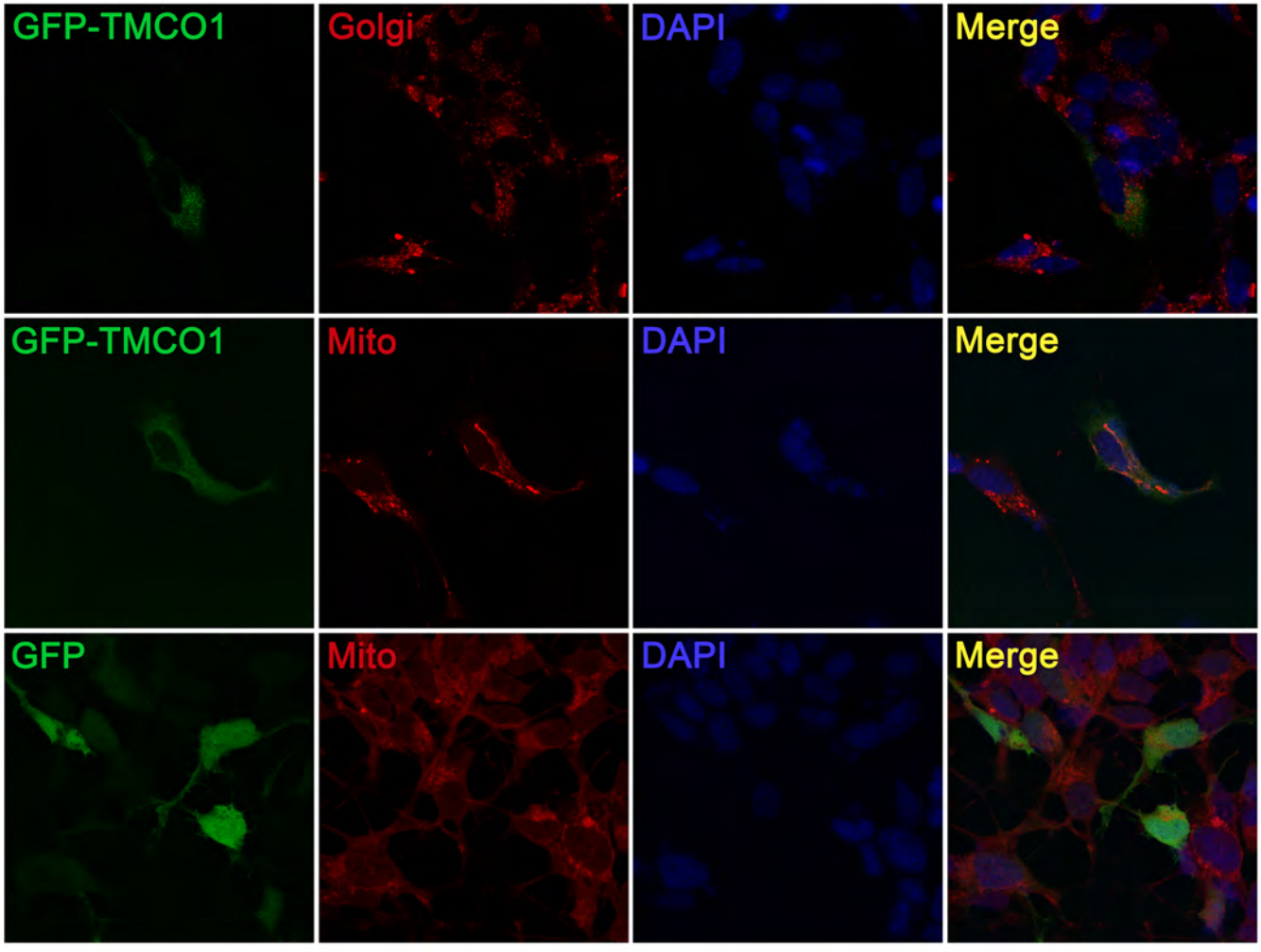
GFP-TMCO1
Golgi
DAPI
Merge
GFP-TMCO1
Mito
DAPI
Merge
GFP
Mito
DAPI
Merge

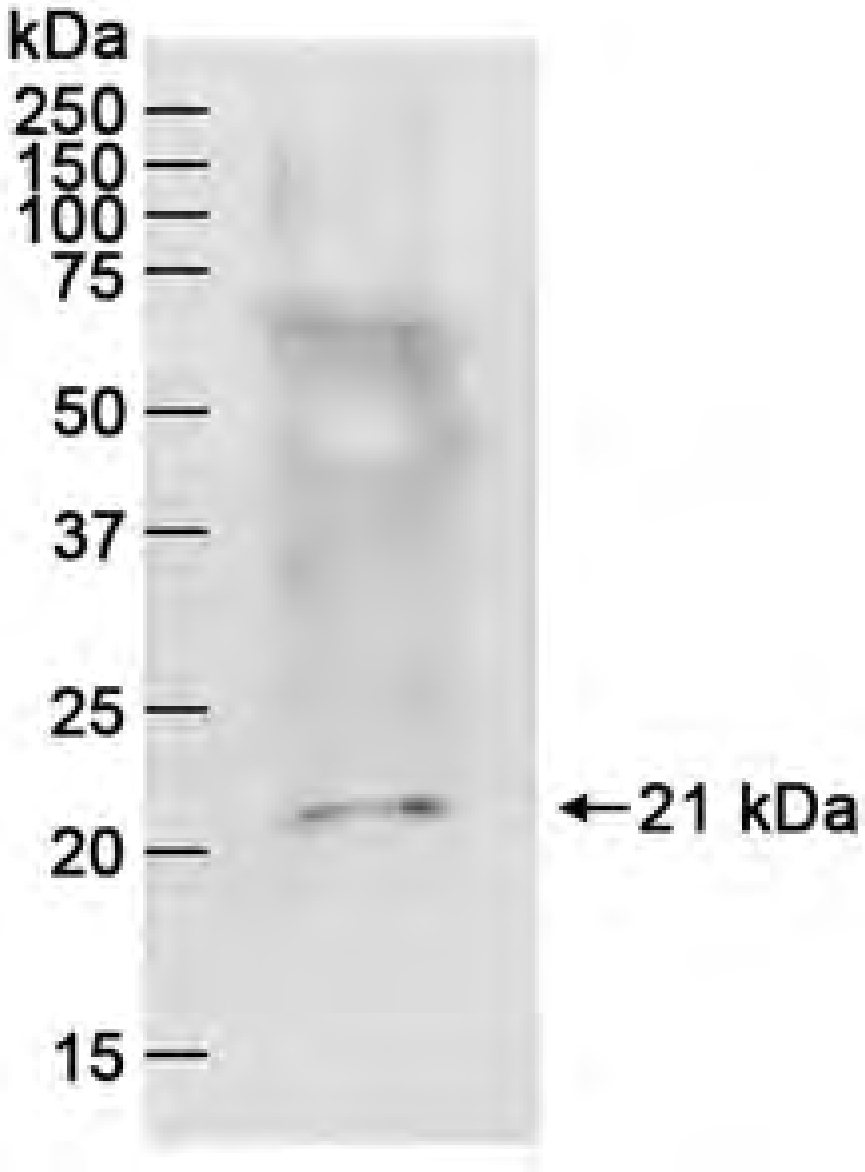
kDa
250
150
100
75
50
37
25
20
15
21 kDa

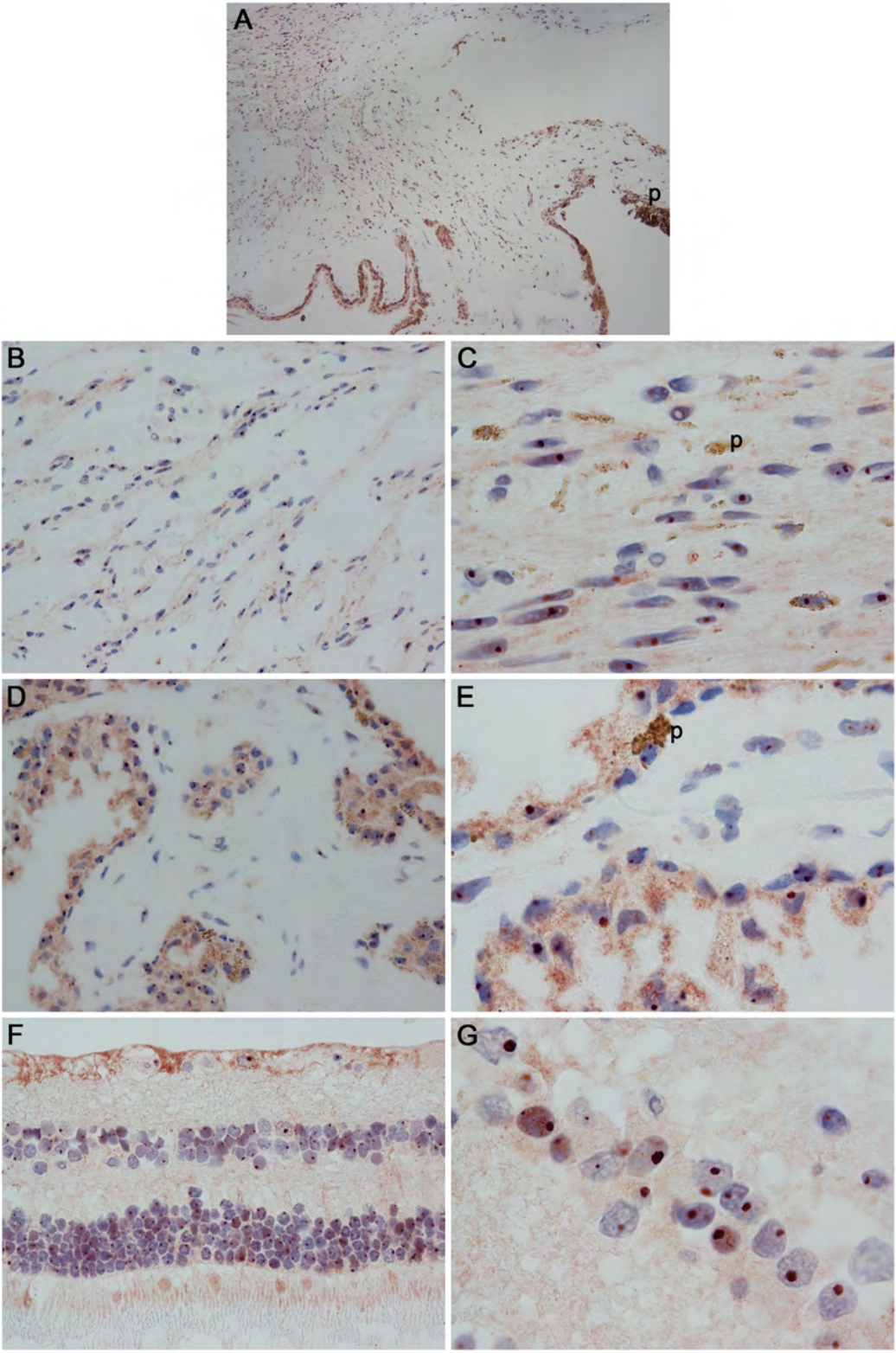
A
p
B
C
p
D
E
p
F
G

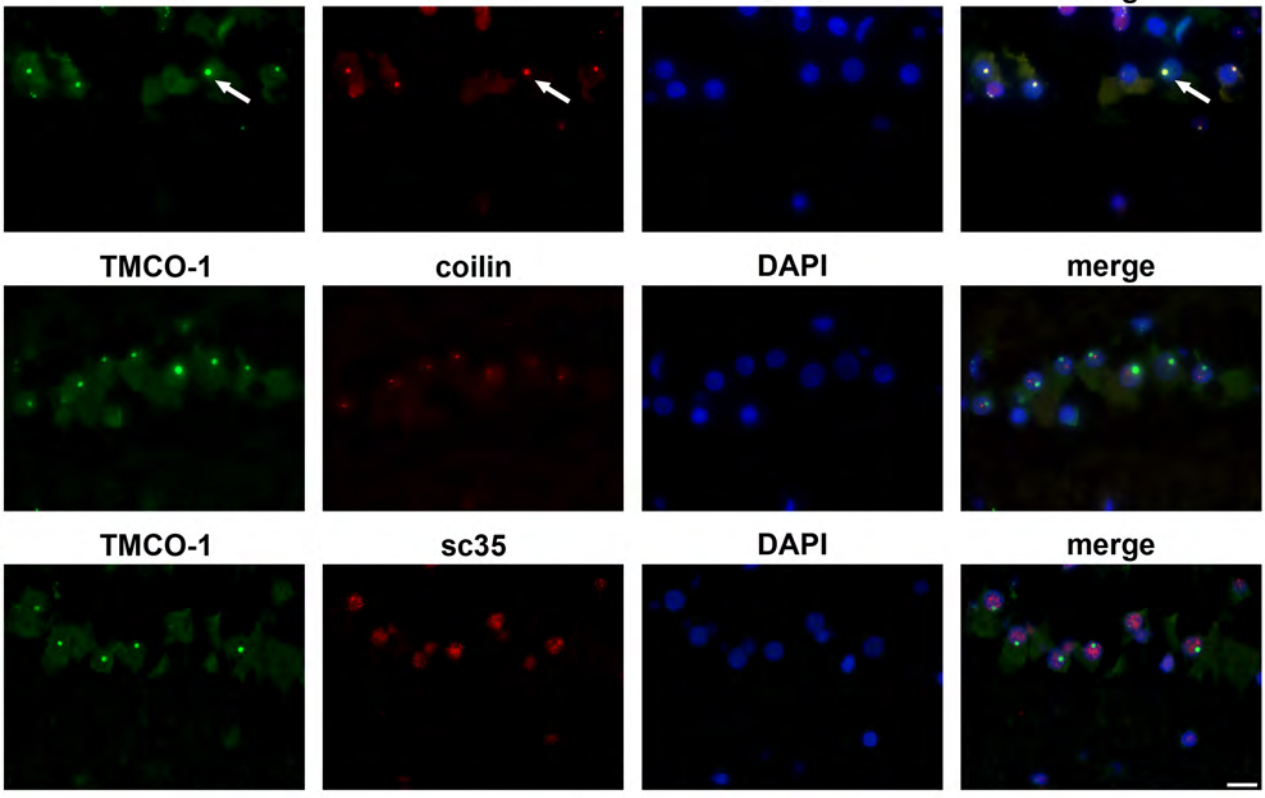
TMCO-1
nucleolin
DAPI
merge
TMCO-1
coilin
DAPI
merge
TMCO-1
sc35
DAPI
merge

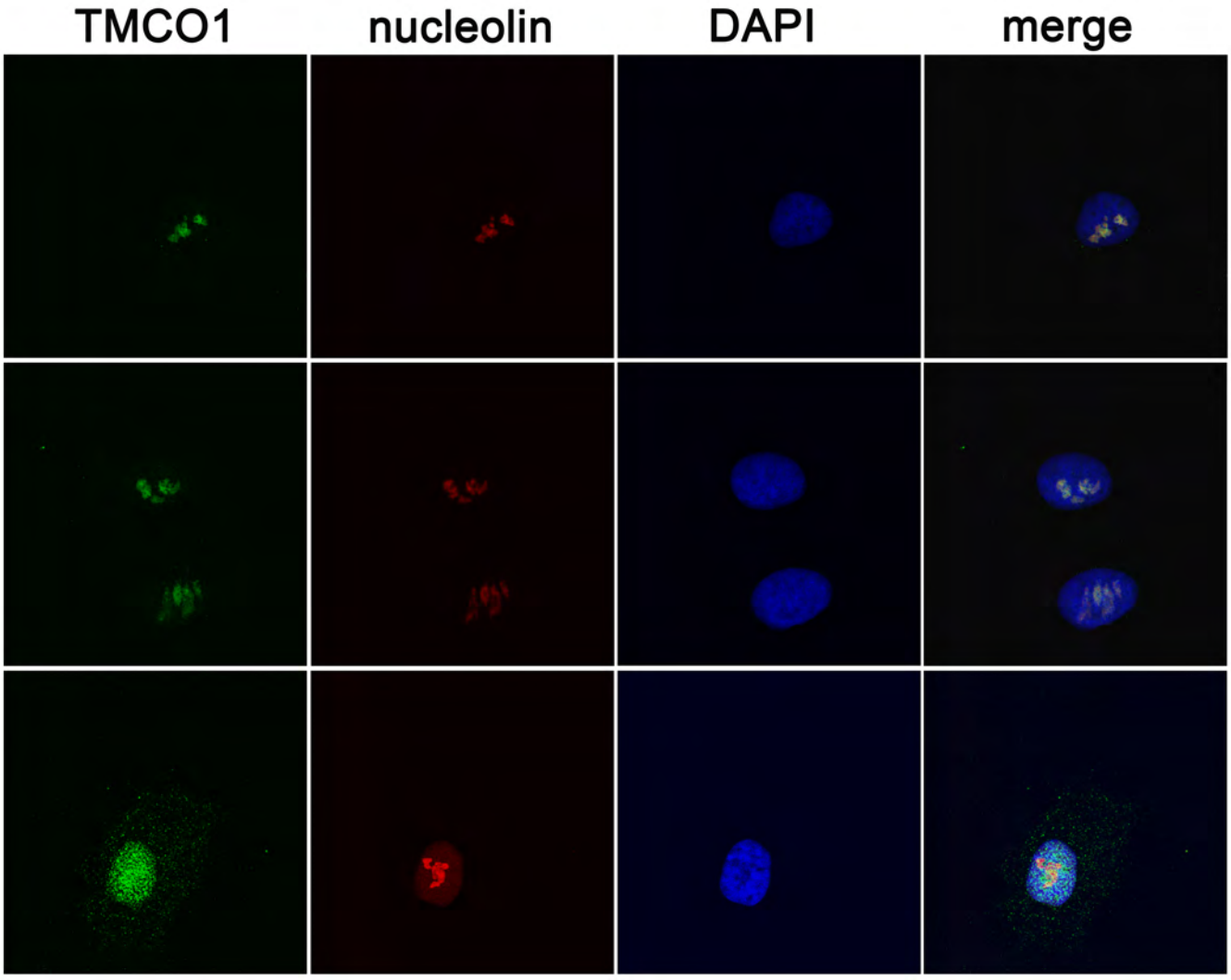
TMCO1
nucleolin
DAPI
merge